Facile fabrication of SiC/ZnO composite and its enhanced sensitivity for detection of NO

Cite as: AIP Advances 13, 105218 (2023); doi: 10.1063/5.0165054
Submitted: 3 July 2023 • Accepted: 12 September 2023 •
Published Online: 13 October 2023

Jun Zhang,[1,a] Yu Cui,[1] Yi Lin,[1] Yalu Tang,[1] Yanlong Yu,[1] Sai Yan,[1] Benling Gao,[1] Guang Hu,[1] and Paul K. Chu[2,a]

AFFILIATIONS

[1] Faculty of Mathematics and Physics, Huaiyin Institute of Technology, Huaian 223003, China
[2] Department of Physics, Department of Materials Science and Engineering, and Department of Biomedical Engineering, City University of Hong Kong, Tat Chee Avenue, Kowloon, Hong Kong, China

[a] **Authors to whom correspondence should be addressed:** zhangjun@hyit.edu.cn and paul.chu@cityu.edu.hk

ABSTRACT

Zinc oxide (ZnO) is an attractive material for gas sensors, and various ZnO-based sensors have been developed to detect gas pollution. In this work, a series of SiC/ZnO composites were fabricated by incorporating silicon carbide nanocrystals (SiC NCs) into ZnO microspheres by a grinding method. The SiC/ZnO composite exhibited a significantly enhanced gas sensitivity response toward NO gas in comparison to ZnO. The test revealed that the response of the composite was 251.1 for 100 ppm of nitrogen monoxide (NO), and the detection limit was as low as 100 ppb. Through spectral and comparative analyses, it has been indicated that the active functional groups of the SiC NCs have a substantial impact on the detection of NO, and the corresponding mechanism is studied and discussed. This work offers a simple strategy for the fabrication of SiC/ZnO material with enhanced sensitivity in sensing applications.

I. INTRODUCTION

Increasing energy consumption has exacerbated the emission of toxic gases such as nitrogen oxides (NO and NO_2), carbon oxides (CO and CO_2), sulfur oxides (SO and SO_2), ammonia (NH_3), and so on, which pose increasing threats to the environment and human health.[1] As a harmful gas, NO is produced during combustion in automobile engines. This gas poses a threat to human health and can easily oxidize into nitrogen dioxide (NO_2) even at ambient temperatures.[2,3] Therefore, the expeditious and accurate detection of NO is of significant importance in environmental protection. Numerous studies have been conducted to investigate sensors for NO,[4,5] and in particular, metal oxides (MOs) such as SnO_2, ZnO, WO_3, and In_2O_3 have been incorporated into NO gas sensors. These MO materials are stable and can offer good gas sensing response characteristics.[6–9]

As a wide bandgap semiconductor, ZnO offers advantages such as low cost, high sensitivity, ease of preparation, and compatibility with electronic devices, which enable the fabrication of affordable and compact ZnO-based gas sensors.[10,11] Nevertheless, the gas sensing material still has some disadvantages, such as low selectivity and high operating temperatures, which impede its use in applications. To improve the performance of gas sensors, several studies have concentrated on the development of novel sensitive materials and the synthesis of composite systems of ZnO with other materials.[12–14] Therefore, the development of gas-sensitive materials with good selectivity and stability and high sensitivity is still of significance for the application of sensors.

The unique physical and chemical characteristics of silicon carbide (SiC) have aroused scientific interest in the gas-sensing field for many years. Some works reported that MO/SiC composite materials showed good stability and a high response to specific gases.[15,16] According to prior research, there exist abundant O species on the surface of SiC nanocrystals (SiC NCs) prepared by acid etching. The O species have a strong impact on the properties of SiC, thereby enabling its utilization in diverse domains.[17–19] Based on the

aforementioned research, it can be said that specific surface functional groups on SiC NCs have the potential to selectively interact with particular gases, which makes it a promising option for enhancing the sensitivity of various materials. In this study, a SiC/ZnO composite has been successfully fabricated. The material exhibits remarkable selectivity toward NO gas, along with rapid response and recovery times. The sensitivity response of the composite is significantly enhanced compared to ZnO, and the mechanism has been thoroughly examined and discussed.

II. SYNTHESIS

ZnO microspheres were synthesized by the hydrothermal method.[20] In brief, 0.4 mmol $Na_2SO_4 \cdot 10\ H_2O$ and 0.6 mmol $Zn(CH_3COO)_2 \cdot 2H_2O$ were dissolved in 4 ml of deionized water and 5 ml of ethanol, and 1.8 mmol glycine was added dropwise and stirred for 20 minutes. Then, 3.3 mmol NaOH was added and magnetically stirred for 30 min. Finally, the white gel was transferred to a 20 ml autoclave and heated at 180 °C for 8 h in a thermostat. The final product was collected and washed with deionized water, followed by calcination at a temperature of 400 °C for 2 h.

3C-SiC NCs were prepared by acid etching.[17] In brief, 6.0 g of 3C-SiC powder was added to a mixture containing 15 ml of 65 wt. % nitric acid (HNO_3) and 45 ml of 40 wt. % hydrofluoric acid (HF). After reaction at 100 °C for 1 h, the precipitate was collected and centrifuged. Following the washing and drying process, 30 ml of deionized water was added to the precipitate and sonicated for about 1 h. Then the supernatant containing 3C-SiC NCs was collected by centrifugation. After being neutralized with sodium hydroxide (NaOH), the solution of 3C-SiC NCs was obtained by dialysis.

The solutions with different amounts of SiC (3.0, 6.0, and 20.0 mg SiC NCs) were mixed with 100 mg of ZnO powder and ball-milled for 1 h. During the grinding process, 100 μl of deionized water was used as a dispersant. The composites containing 3.0, 6.0, and 20.0 mg of SiC NCs were labeled as SiC-1/ZnO, SiC-2/ZnO, and SiC-3/ZnO, respectively. Finally, the composites were coated on a ceramic tube with gold electrodes. After being cured at 150 °C for 1 h, a nickel–chromium (Ni–Cr) wire was inserted into the ceramic tube. The ceramic tube and wire were welded onto a hexagonal base to prepare the sensor. The sensors fabricated with SiC-1/ZnO, SiC-2/ZnO, and SiC-3/ZnO were denoted as device-1, device-2, and device-3, respectively.

III. CHARACTERIZATION

X-ray diffraction (XRD) analysis was conducted using a 40 KV/200 mA setup with Cu Kα radiation (XRD, X'PERT, PANalytical). The microstructures and morphologies of the composites were examined on a transmission electron microscope (HR-TEM, JEOL JEM-4000EX). The x-ray photoelectron spectra (XPS) were obtained with a K-Alpha spectrometer (Thermo Fisher Scientific Corporation) equipped with an Al Kα x-ray source.

IV. RESULTS AND DISCUSSION

The morphologies and surface structures of the samples are depicted in Fig. 1. Figure 1(a) shows that the SiC NCs have a size of 3–5 nm, and the inset shows the typical interplanar spacing of 0.25 nm, which corresponds to the (111) plane of 3C-SiC.[17] Fig. 1(b) shows that the ZnO has a microsphere morphology with a rough surface and that the diameter of these microspheres is about 2 μm. Figures 1(c), 1(e), and 1(g) are TEM images of SiC-1/ZnO, SiC-2/ZnO, and SiC-3/ZnO, respectively. Accordingly, Figs. 1(d), 1(f), and 1(h) provide the high-resolution TEM images of SiC-1/ZnO, SiC-2/ZnO, and SiC-3/ZnO, respectively. As seen in Figs. 1(c), 1(e), and 1(g), the samples show no obvious differences compared to ZnO. From the high-resolution TEM images shown in Figs. 1(d), 1(f), and 1(h), the SiC NCs can be distinguished from ZnO. The interlayer spacing of 0.28 nm corresponds to the (100) plane of ZnO,[21] while that of 0.25 nm is in good agreement with the (111) plane of 3C-SiC. The existence of SiC is also confirmed by the XPS spectra depicted in Fig. S1 of the ADV23-AR-02182 / v13i10 supplementary material.

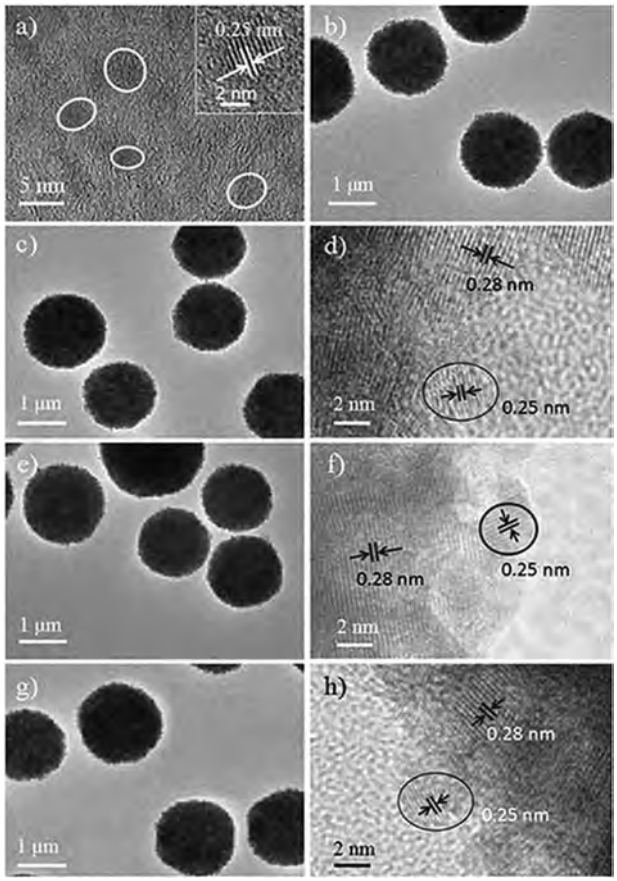

FIG. 1. (a) TEM and HRTEM (inset) images of the SiC NCs; (b) TEM images of ZnS microspheres; (c) TEM and (d) HRTEM images of SiC-1/ZnO; (e)–(h) TEM and HRTEM images of SiC-2/ZnO and SiC-3/ZnO, respectively.

Figure 2 shows the XRD patterns. As seen, ZnO exhibits distinct peaks at 31.7°, 34.4°, and 36.2° from the (100), (002), and (101) planes (JCPDS No. 36-1451), respectively, which demonstrates that the ZnO has a wurtzite hexagonal structure.[20] There are no distinct SiC peaks in the XRD patterns of the SiC/ZnO composites; the

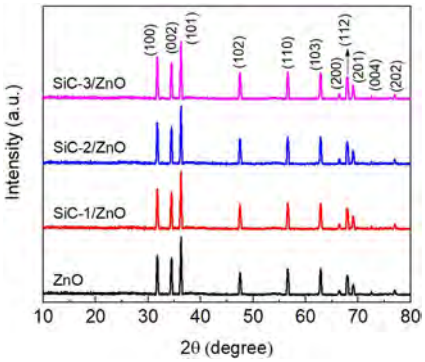

FIG. 2. XRD patterns of the samples.

reason may be that the SiC NCs are very small and uniformly distributed on the ZnO microspheres. To evaluate the crystallinity of ZnO, the Debye–Scherrer equation is adopted,[20,22]

$$D = \frac{K\lambda}{\beta \cos \theta},$$

where D is the grain diameter derived from the peaks at 31.7°, 34.4°, and 36.2°; β is the full-width at half-maximum (FWHM); K is the Debye–Scherrer constant, equal to 0.89; λ is 1.5406 Å for Cu Kα x rays; and θ is the diffraction angle. The mean grain size is calculated to be 36.3 nm, significantly larger than the size of the SiC NCs.

Figure 3 shows the XPS spectra of the samples in the O 1s region. As seen, each of the O 1s contains two components. The peak at 530.1 eV can be attributed to the lattice oxygen in ZnO, while the higher energy peak at 531.7 eV is indicative of oxygen species located on the surface of ZnO. These surface oxygen species encompass different forms of chemisorbed oxygen and hydroxy groups (−OH).[15,23,24] In all of the SiC/ZnO samples, the proportion of O species is higher than that of ZnO, potentially attributed to the

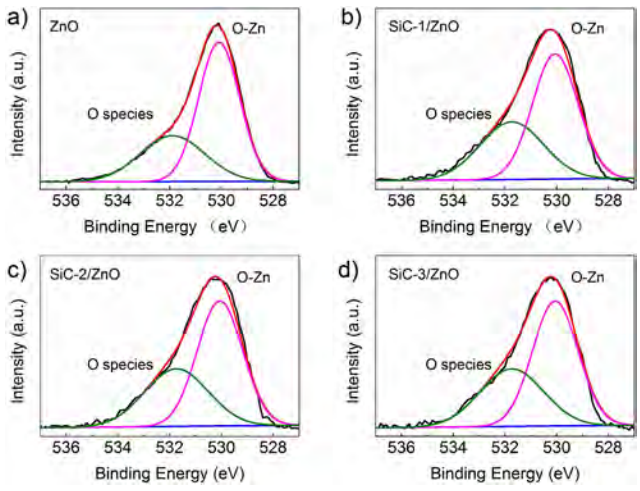

FIG. 3. XPS spectra of (a) ZnO, (b) SiC-1/ZnO, (c) SiC-2/ZnO, and (d) SiC-3/ZnO in the O 1s region.

elevated concentration of oxygen surface species.[15,23] The Zn 2p XPS spectra of the samples are depicted in Fig. S2 of the supplementary material. There are no discernible alterations observed in the Zn 2p XPS spectra of ZnO/SiC nanocomposites compared to the corresponding spectrum of ZnO. This implies that there were no observed changes in the ZnO substance, which aligns with the findings of the XRD analysis.

The composites were made into sensing devices to determine the gas sensing performance, as shown in Fig. 4(a). The setup consists of a gas chamber, Fluke 8846A digital multimeter, and GPD3303S DC power supply. The operating temperature is controlled by the Ni–Cr wire in the ceramic tube. According to the data presented in Fig. 4(b), device-2 exhibits the highest response of 251.1 at a temperature of 100 °C. In contrast, device-1 and device-3 show the best values of 87 and 56 at 110 °C, respectively. It is worth noting that the best response of ZnO at 96 °C is only 2.8. This discrepancy highlights that the performance of the devices composed of SiC/ZnO is superior to that of pure ZnO. According to the comparative analysis presented in Fig. S3 of the supplementary material, it is hypothesized that the presence of active functional groups, such as −OH,[17,19] on the SiC NCs contributes to the enhancement of sensitivity. The presence of the −OH is verified by the XPS spectra depicted in Fig. S4 of the supplementary material. The degradation in the performance of device-3 may be attributed to the increased presence of SiC NCs, which in turn increases the static resistance of the composite, thus affecting the resistance beyond the resistance change when NO is present.[20]

In addition, the SiC/ZnO composite exhibits excellent selectivity for NO in the presence of other gases such as NH_3, NO_2, SO_2, and H_2S. Figure 4(c) shows that the response to the other gases is poorer due to the different reactions between the active functional groups of SiC and NO. Figure 4(d) shows the response and recovery curve of device-2 when exposed to 100 ppm of NO at 100 °C. Usually, the response and recovery time is defined as the time required to attain 90% of the final stable resistance.[25] According to Fig. 4(d), the response time and the recovery time are 32 and 33 s, respectively. The quick recovery/response suggests that a surface reaction that is reversible takes place during gas detection.[20]

Figure 5(a) shows the dynamic response of device-2 at 100 °C and NO concentrations ranging from 100 ppb to 100 ppm. As seen in Fig. 5(a), the response is directly correlated with the gas concentration; the higher the gas concentration, the stronger the response. In addition, even at a concentration as low as 100 ppb, the response is still noticeable, as shown in the inset. Furthermore, device-2 exhibits a linear correlation between the response and gas concentration, as depicted in Fig. 5(b), suggesting the possibility of accurate quantitative detection of NO. Figure 5(c) depicts the dynamic response curves of five intake and exhaust gas processes of device-2 at 100 °C. It is evident that the curve exhibits a notable consistency, suggesting that the device has robust consistency and repeatability. The long-term stability assessment is depicted in Fig. 5(d). In the span of 10 days, there is no obvious decline in the response due to the robustness and strong oxidation resistance of SiC NCs during repeated cycles of cooling and heating.

The classical electron depletion layer mechanism can be applied to elucidate the response process.[20,26,27] As is known, ZnO is an n-type semiconductor, and an external stimulus promotes electrons to the conduction band to form carriers in the device. When the

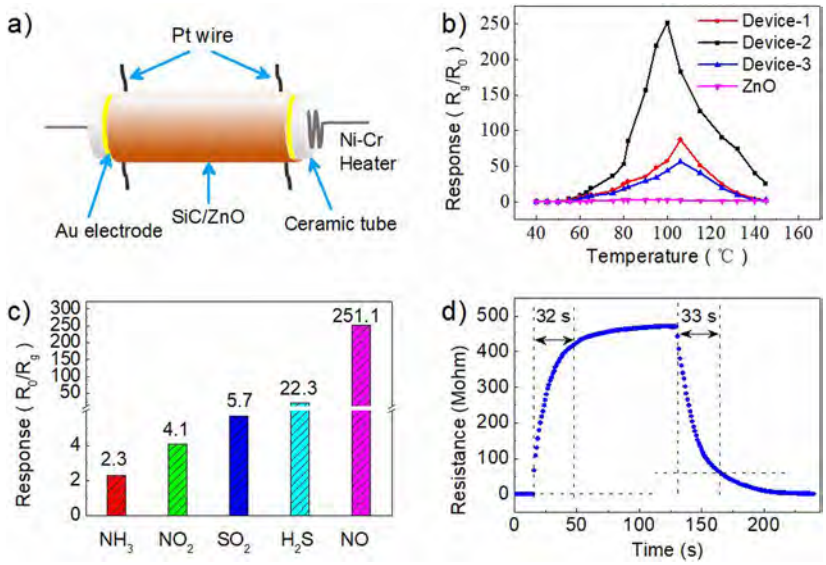

FIG. 4. (a) Schematic of the device. (b) Responses of the devices to 100 ppm NO at different temperatures. (c) Selectivity of device-2 to 100 ppm of different gases. (d) Response and recovery time of device-2 to 100 ppm of NO gas at 100 °C.

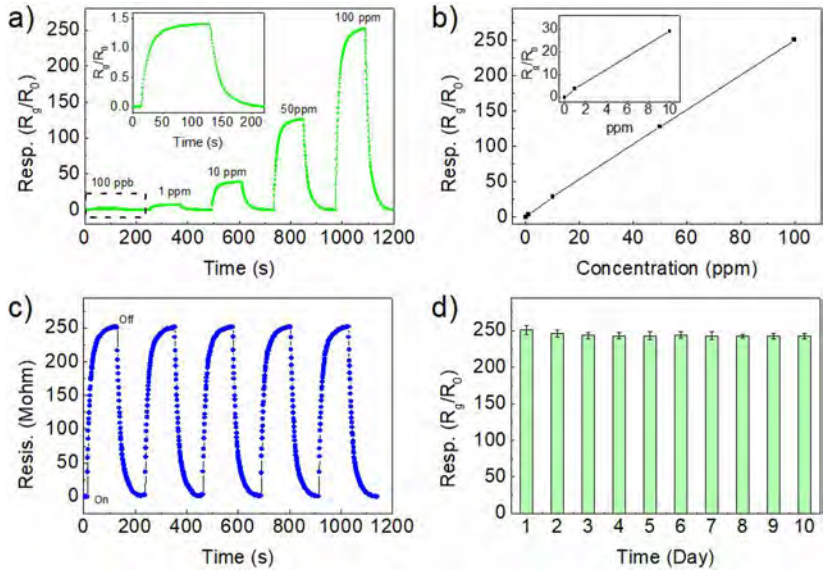

FIG. 5. (a) Dynamic response curve and (b) the response of device-2 to 100 ppb–100 ppm of NO at 100 °C. (c) Repeatability curve and (d) long-term stability of device-2 to 100 ppm of NO at 100 °C.

device is exposed to oxidizing gases, such as oxygen in the air, the gas molecules adsorbed on the surface may assimilate the free electrons. The loss of free electrons results in the formation of an electron depletion layer and a decrease in conductivity. If the sensor is then exposed to a reducing gas, the reducing gas may react with the oxygen groups on the surface and release electrons. This process decreases the electron depletion layer and restores conductivity. Using oxygen as the adsorbing molecule, the chemical reaction that takes place on the material's surface can be elucidated as

$$O_2(\text{ads}) + e^- \rightarrow O_2^-(\text{ads}), \quad (1)$$

$$O_2^-(\text{ads}) + e^- \rightarrow 2O^-(\text{ads}), \quad (2)$$

$$O^-(\text{ads}) + e^- \rightarrow O^{2-}(\text{ads}). \quad (3)$$

Reactions (2) and (3) occur at temperatures above 150 °C,[12,28] but reaction (1) typically takes place below 150 °C.[20,29] Pure ZnO

microspheres show a weak reaction to NO, suggesting that the surface hardly undergoes traditional adsorption reaction [Fig. 4(b)]. However, for the SiC/ZnO composite, the NO response is improved, indicating that the doped SiC NCs play a significant role in the sensitivity. NO is highly active, and the unpaired electron facilitates the formation of nitric oxide free radicals. It is worth noting that although NO_2 possesses the capacity to receive electrons, it cannot create $^{\cdot}NO$ without external stimulation.

As previously investigated, there are affluent active functional groups on the surface of SiC NCs such as hydroxyl and amino groups, which may be produced by acidification and activation by surface reactions.[17–19,30] Since the gas sensing experiments here were conducted at a temperature below 150 °C, the −OH on the SiC NCs is retained and it is believed that the $^{\cdot}NO$ reacts with the −OH as follows:

$$SiC - OH + \bullet ON \rightleftarrows HNO(ads) + SiC - O\bullet . \quad (4)$$

The radical SiC–O• is produced as an intermediate product. It possesses an oxidation potential and exhibits a strong inclination toward electron capture. In the SiC/ZnO composite, the free electrons in the conduction band of ZnO may be trapped as follows:

$$SiC - O\bullet + e^{-} \rightarrow SiC - O^{-}. \quad (5)$$

By decreasing the concentration of carriers, the conductivity of the composite decreases, and the resistance increases. The composite shows a limited response to oxidizing gas, suggesting that direct removal of carriers from the composite by the oxidizing gas is challenging during the chemical adsorption process. The presence of SiC NCs in the composite material facilitates the conversion of the gas adsorption reaction into a solid-phase contact reaction. This transformation makes electron transfer more ready in the reaction. Furthermore, the morphology of the materials determines the gas-sensing efficacy. Materials possessing a rough micro-morphology have a larger surface area and surface energy, which leads to higher affinity to oxygen and target gas molecules for more pronounced gas-sensing responses. The composite indeed has a microspherical morphology with a large surface area; therefore, the interaction with NO is enhanced. In addition, the functional groups on the SiC NCs offer more reaction sites, thereby enhancing the sensitivity of the material toward NO.

V. CONCLUSION

In summary, ZnO microspheres were prepared by a hydrothermal method, followed by incorporation of SiC NCs into ZnO by the grinding method to produce the SiC/ZnO composite. The device composed of the SiC/ZnO composite exhibits great sensitivity to NO gas, along with excellent selectivity. The study also analyzed the mechanism of SiC/ZnO and determined that SiC NCs have a notable impact on the gas sensitivity toward NO. The incorporation of SiC NCs into ZnO materials has the potential to serve as a novel approach for improving the gas-sensing capabilities of sensitive materials for detection of NO.

SUPPLEMENTARY MATERIAL

See the supplementary material for the XPS spectra of the samples and the gas sensitive responses of ZnO to different gases.

AUTHOR DECLARATIONS

Conflict of Interest

The authors have no conflicts to disclose.

Author Contributions

Jun Zhang: Conceptualization (equal); Formal analysis (equal). **Yu Cui**: Data curation (equal); Formal analysis (equal); Writing – original draft (equal). **Yi. Lin**: Formal analysis (equal); Methodology (equal). **Yalu Tang**: Methodology (equal); Resources (equal). **Yanlong Yu**: Formal analysis (equal); Resources (equal). **Sai Yan**: Investigation (equal); Methodology (equal). **Benling Gao**: Data curation (equal); Resources (equal). **Guang Hu**: Data curation (equal); Formal analysis (equal). **Paul K. Chu**: Conceptualization (equal); Writing – review & editing (equal).

DATA AVAILABILITY

The data that support the findings of this study are available within the article and the supplementary material.

REFERENCES

[1] J. Zhang, X. Jia, T. Liu, J. Yang, S. Wang, Y. Li, D. Shao, L. Feng, and H. Song, Sens. Actuators, B **359**, 131601 (2022).
[2] Q. Li, W. Zeng, and Y. Li, Sens. Actuators, B **359**, 131579 (2022).
[3] J. H. Bang, A. Mirzaei, S. Han, H. Y. Lee, K. Y. Shin, S. S. Kim, and H. W. Kim, Ceram. Int. **47**, 5099–5111 (2021).
[4] P. Raju and Q. Li, J. Electrochem. Soc. **169**, 057518 (2022).
[5] T. Y. Chang, A. K. Singh, J. H. Shao, C. Y. Huang, J. M. Shieh, D. S. Wuu, P.-L. Liu, and R.-H. Horng, Appl. Surf. Sci. **637**, 157929 (2023).
[6] P. Su, W. Li, J. Zhang, and X. Xie, Vacuum **199**, 110961 (2022).
[7] B. Soltabayev, G. Yergaliuly, A. Ajjaq, A. Beldeubayev, S. Acar, Z. Bakenov, and A. Mentbayeva, ACS Appl. Mater. Interfaces **14**(36), 41555–41570 (2022).
[8] L. Yang, A. Marikutsa, M. Rumyantseva, E. Konstantinova, N. Khmelevsky, and A. Gaskov, Sensors **19**, 3405 (2019).
[9] N. Zhao, J. Feng, Q. Chen, J. Li, X. Ge, B. Zhao, P. Yuan, L. Fang, and L. Yin, New J. Chem. **47**, 1715–1723 (2023).
[10] P. J. Cao, Y. Z. Cai, D. Pawar, S. Han, W. Y. Xu, M. Fang, X. K. Liu, Y. X. Zeng, W. J. Liu, Y. M. Lu, and D. L. Zhu, J. Mater. Chem. C **10**, 4295–4305 (2022).
[11] X. Chang, X. R. Qiao, K. Li, P. Wang, Y. Xiong, X. Li, F. Xia, and Q. Xue, Sens. Actuators, B **317**, 128208 (2020).
[12] N. Yamazoe and K. Shimanoe, Sens. Actuators, B **138**, 100–107 (2009).
[13] Y. Fang, D. D. Yang, C. Y. Xiang, M. Shi, H. Zhao, and H. Asadi, J. Mol. Graphics Modell. **99**, 107630 (2020).
[14] H. R. Yousefi, B. Hashemi, A. Mirzaei, H. Roshan, and M. H. Sheikhi, Mater. Sci. Semicond. Process. **117**, 105172 (2020).
[15] V. B. Platonov, M. N. Rumyantseva, A. S. Frolov, A. D. Yapryntsev, and A. M. Gaskov, Beilstein J. Nanotechnol. **10**, 1537–1547 (2019).
[16] H. Zhang, S. Ju, X. Jin, Y. Yuan, Y. Wu, A. K. Nadda, A. Pugazhendhi, L. Cai, and C. Xia, Renewable Sustainable Energy Rev. **169**, 112915 (2022).
[17] X. L. Wu, S. J. Xiong, J. Zhu, J. Wang, J. C. Shen, and P. K. Chu, Nano Lett. **9**, 4053 (2009).

[18]J. Wang, S. J. Xiong, X. L. Wu, T. H. Li, and P. K. Chu, Nano Lett. **10**, 1466 (2010).
[19]C. He, X. Wu, J. Shen, and P. K. Chu, Nano Lett. **12**, 1545 (2012).
[20]Z. Yu, L. Zhang, X. Wang, D. He, H. Suo, and C. Zhao, Sensors **20**, 4961 (2020).
[21]T. Shi, H. Hou, S. Hussain, C. Ge, M. A. Alsaiari, A. S. Alkorbi, G. Liu, R. Alsaiari, and G. Qiao, Chemosphere **287**, 132178 (2022).
[22]S. Li, L. Zhang, M. Zhu, G. Ji, L. Zhao, J. Yin, and L. Bie, Sens. Actuators, B **249**, 611–623 (2017).
[23]L. Chen, Z. Liu, S. Bai, K. Zhang, D. Li, A. Chen, and C. Liu, Sens. Actuators, B: Chem. **143**(2), 620–628 (2010).
[24]M. Chen, X. Wang, Y. H. Yu, Z. L. Pei, X. D. Bai, C. Sun, R. F. Huang, and L. S. Wen, Appl. Surf. Sci. **158**, 134–140 (2000).
[25]Y. Liu, F. Liu, J. Bai, T. Liu, Z. Yu, M. Dai, L. Zhou, H. Wang, Y. Zhang, H. Suo, and G. Lu, Sens. Actuators, B **296**, 126619 (2019).
[26]D. Miller, S. Akbar, and P. Morris, Sens. Actuators, B **204**, 250–272 (2014).
[27]J. Yu, S. Ippolito, W. Wlodarski, M. Strano, and K. Kalantarzadeh, Nanotechnology **21**, 265502 (2010).
[28]O. Lupan, V. V. Ursaki, G. Chai, L. Chow, G. A. Emelchenko, I. M. Tiginyanu, A. N. Gruzintsev, and A. N. Redkin, Sens. Actuators, B **144**, 56–66 (2010).
[29]S.-C. Chang, J. Vac. Sci. Technol. **17**, 366–369 (1980).
[30]S. J. Schoell, M. Sachsenhauser, A. Oliveros, J. Howgate, M. Stutzmann, M. S. Brandt, C. L. Frewin, S. E. Saddow, and I. D. Sharp, ACS Appl. Mater. Interfaces **5**, 1393–1399 (2013).

Supplementary Materials

Facile Fabrication of SiC/ZnO Composite and its Enhanced Sensitivity for Detection of NO

Jun Zhang[1] *, Yu Cui[1], Yi. Lin[1], Yalu Tang[1], Yanlong Yu[1], Sai Yan[1], Benling Gao[1], Guang Hu[1], Paul K. Chu[2] *

[1] *Faculty of Mathematics and Physics, Huaiyin Institute of Technology, Huaian 223003, China*

[2] *Department of Physics, Department of Materials Science and Engineering, and Department of Biomedical Engineering, City University of Hong Kong, Tat Chee Avenue, Kowloon, Hong Kong, China*

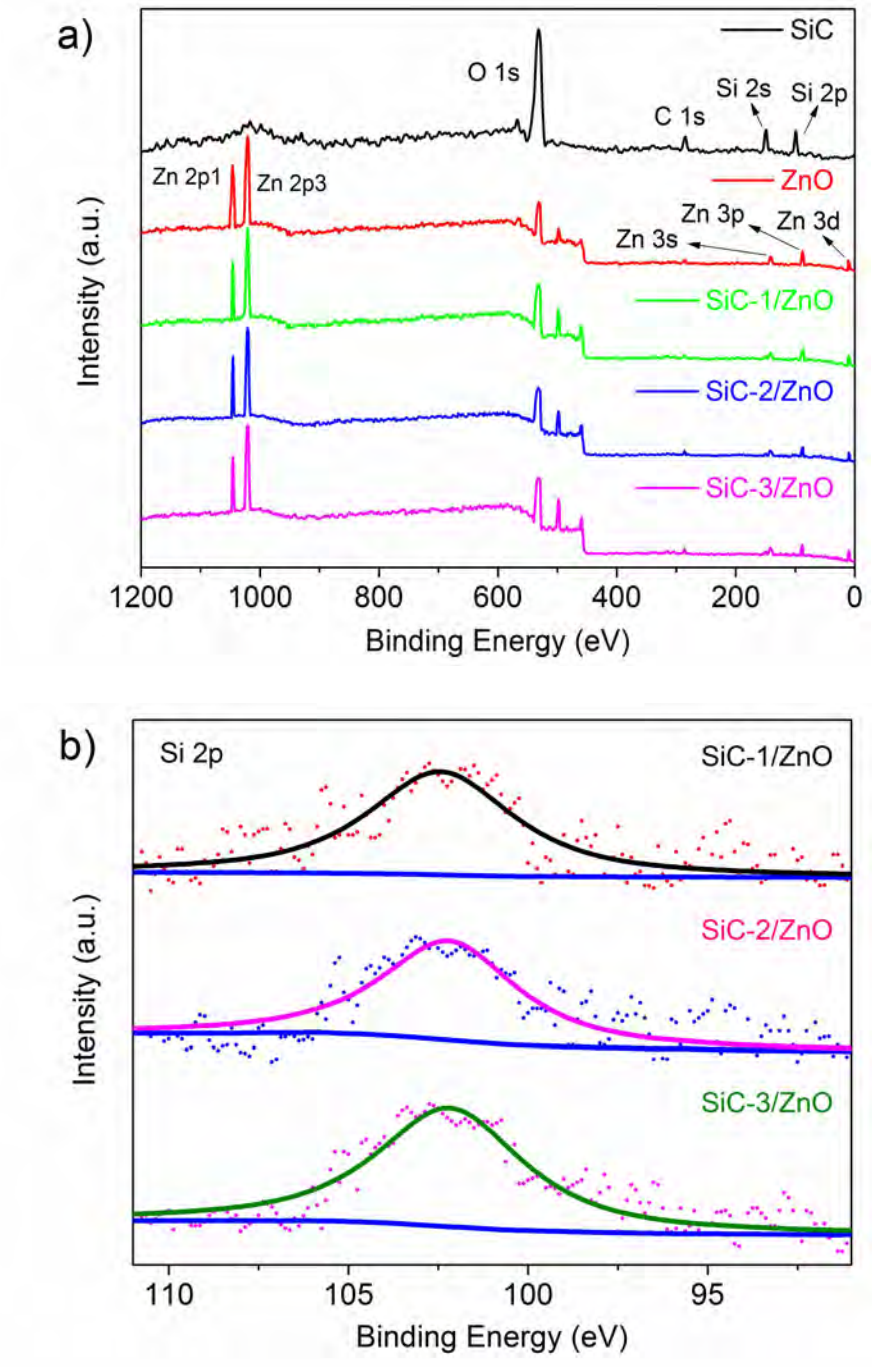

Fig S1. (a) Survey X-ray photoelectron spectra of SiC, ZnO, SiC/ZnO nanocomposites; (b) X-ray photoelectron spectra of SiC/ZnO nanocomposites in the Si 2p region. .

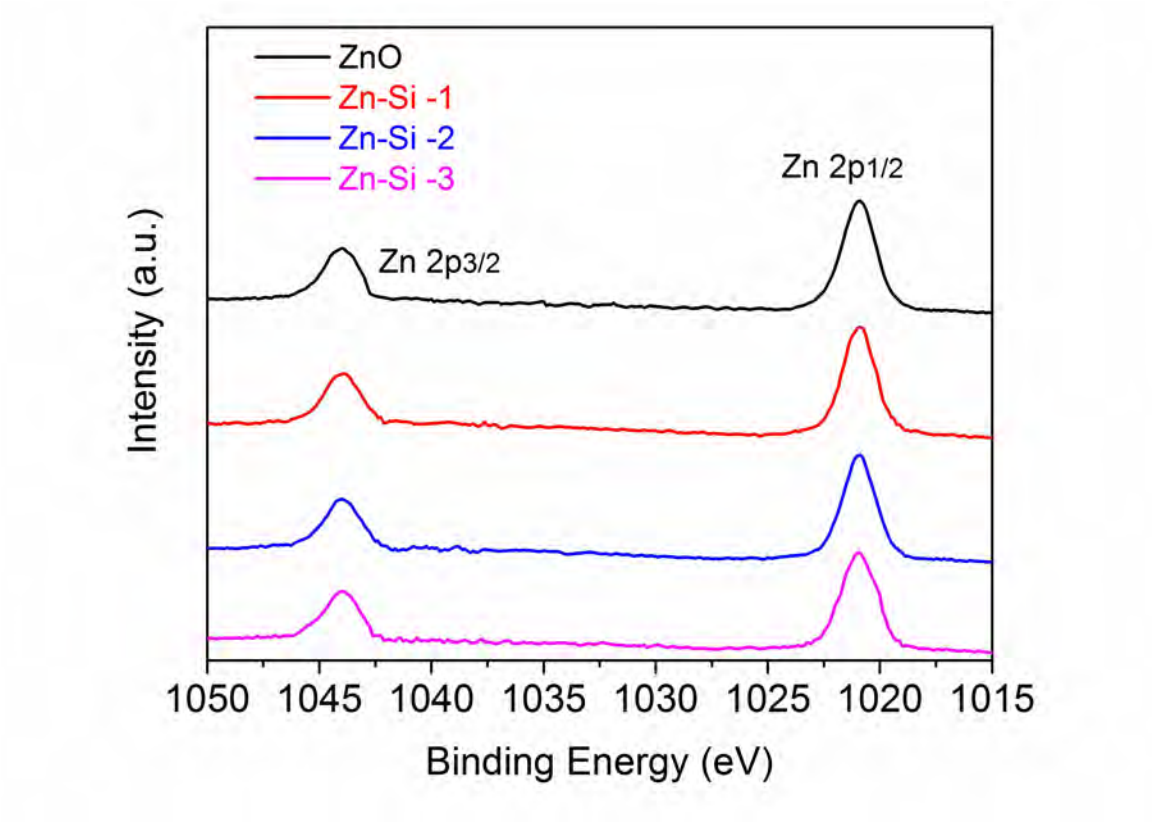

Fig S2. X-ray photoelectron spectra of the samples in the Zn 2p region.

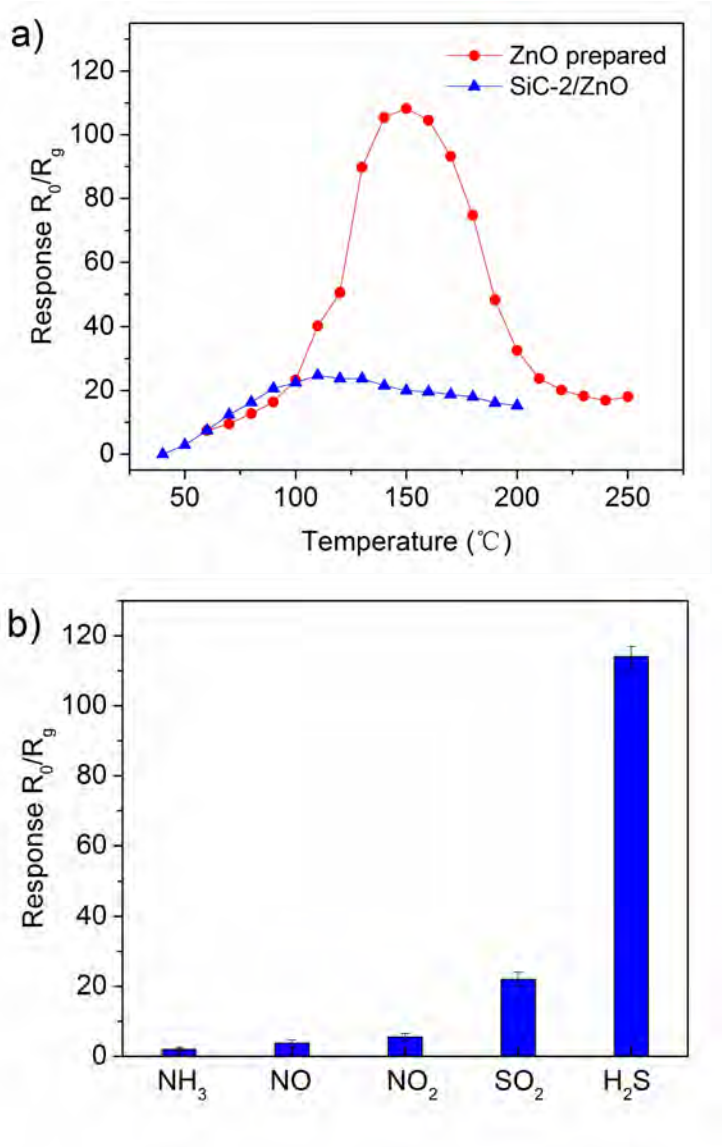

Fig S3. a) The gas sensitive responses of ZnO and Device-2 to 100 ppm H_2S gas at different operating temperature; b) Selectivity of ZnO to different gases at 100 ppm under 150 ℃.

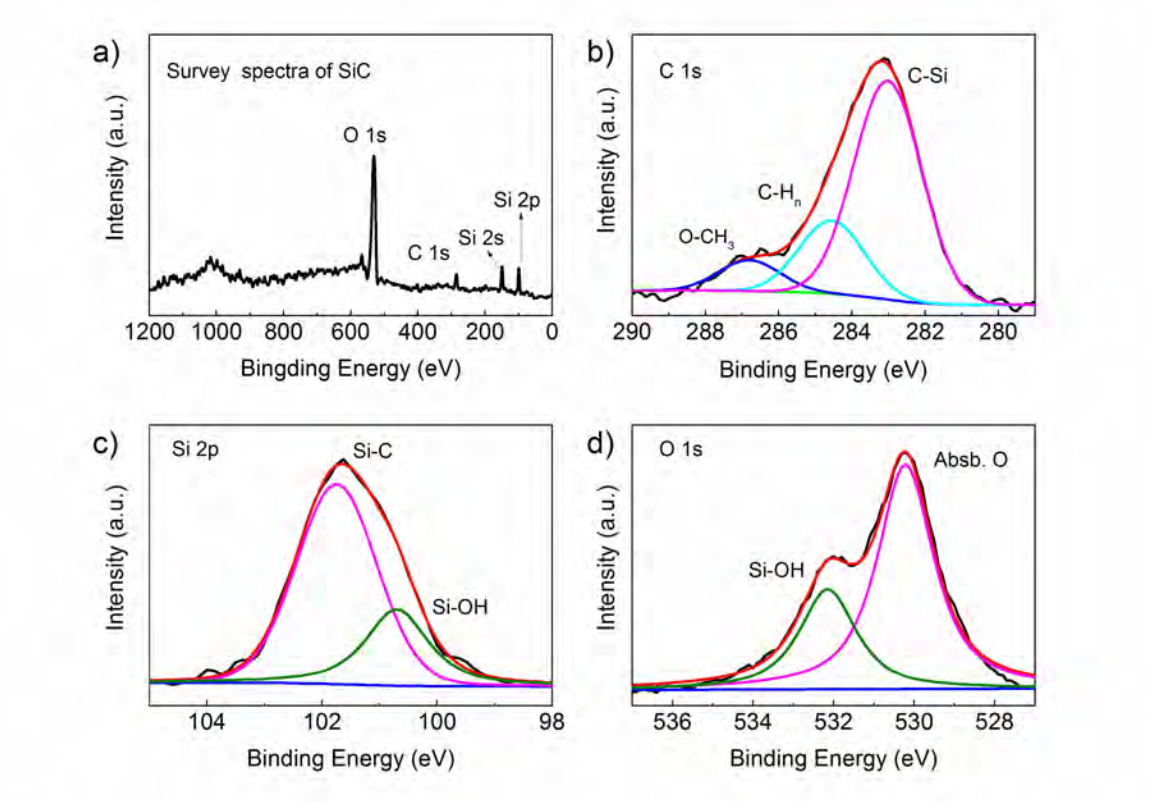

Fig S4. a) Survey X-ray photoelectron spectra of SiC prepared; X-ray photoelectron spectra of the SiC in the C 1s (b), (c) Si 2p, (d) O 1s regions.